JOURNAL OF VIROLOGY, Nov. 2005, p. 14346–14354 Vol. 79, No. 22
0022-538X/05/$08.00+0 doi:10.1128/JVI.79.22.14346–14354.2005

Long Untranslated Regions of the Measles Virus M and F Genes Control Virus Replication and Cytopathogenicity

Makoto Takeda,* Shinji Ohno, Fumio Seki, Yuichiro Nakatsu, Maino Tahara, and Yusuke Yanagi

Department of Virology, Faculty of Medicine, Kyushu University, Fukuoka 812-8582, Japan

Received 24 May 2005/Accepted 23 August 2005

Measles is still a major cause of mortality mainly in developing countries. The causative agent, *measles virus* (MeV), is an enveloped virus having a nonsegmented negative-sense RNA genome, and belongs to the genus *Morbillivirus* of the family *Paramyxoviridae*. One feature of the moribillivirus genomes is that the M and F genes have long untranslated regions (UTRs). The M and F mRNAs of MeV have 426-nucleotide-long 3′ and 583-nucleotide-long 5′ UTRs, respectively. Though these long UTRs occupy as much as ~6.4% of the virus genome, their function remains unknown. To elucidate the role of the long UTRs in the context of virus infection, we used the reverse genetics based on the virulent strain of MeV, and generated a series of recombinant viruses having alterations or deletions in the long UTRs. Our results showed that these long UTRs per se were not essential for MeV replication, but that they regulated MeV replication and cytopathogenicity by modulating the productions of the M and F proteins. The long 3′ UTR of the M mRNA was shown to have the ability to increase the M protein production, promoting virus replication. On the other hand, the long 5′ UTR of the F mRNA was found to possess the capacity to decrease the F protein production, inhibiting virus replication and yet greatly reducing cytopathogenicity. We speculate that the reduction in cytopathogenicity may be advantageous for MeV fitness and survival in nature.

Measles is a highly contagious disease characterized by high fever, cough, and maculopapular rash. The causative agent, *measles virus* (MeV), belongs to the genus *Morbillivirus* of the family *Paramyxoviridae*. The family *Paramyxoviridae* is classified in the order *Mononegavirales*, which is comprised of viruses that have linear nonsegmented single-stranded RNA genomes of negative polarity. Like those of other paramyxoviruses, the MeV genome of 15,894 nucleotides (nt) in length contains six tandem linked genes (some paramyxoviruses have more genes) separated by nontranscribed intergenic (IG) trinucleotides, flanked by a short leader (Le) and a short trailer (Tr) sequence at the 3′ and 5′ end of the genome, respectively (18). The six genes encode nucleocapsid (N), phospho- (P), matrix (M), fusion (F), hemagglutinin (H), and large (L) proteins, respectively. The P gene, exceptionally, encodes additional accessory proteins, V and C proteins, by a process of RNA editing of a cotranscriptional insertion of a single nontemplated G residue and by an alternative translational initiation in a different reading frame, respectively (18, 30). The viral RNA-dependent RNA polymerase is thought to bind the Le sequence at the 3′ terminus of the genome and transcribe respective genes in a sequential and polar manner, by recognizing gene start (GS) and gene end (GE) sequences at each gene boundary (29).

In paramyoviruses, mRNAs generally contain open reading frames (ORFs) with short 5′ and 3′ untranslated regions (UTRs). However, the M and F mRNAs of morbilliviruses have unusually long 3′ and 5′ UTRs, respectively (1, 2, 6, 7, 9, 14, 15, 19, 23, 32, 33, 39, 45). One exception is the canine distemper virus (CDV) F gene. The sequence originally considered as long 5′ UTR was later shown to encode an atypically long leader peptide that modulates the F protein function (47). In MeV, the length of the 3′ UTR of the M mRNA (M 3′ UTR) is 426 nt and that of the 5′ UTR of F mRNA (F 5′ UTR) is 583 nt (6, 39, 42). In the genome, the regions that are transcribed into the M 3′ UTR and F 5′ UTR, combined with the IG trinucleotide, constitute a long stretch of the UTRs of ~1 kb in length between M and F ORFs (Fig. 1A). (In this paper, we indicate the genomic regions by the corresponding regions of mRNA, into which they are transcribed.) Although most morbilliviruses have these long UTRs, the nucleotide sequences are unique among different virus species, and no conserved motifs are found. The only common feature of these long UTRs is the high GC content, and they were suggested to form extensive secondary structures, which may regulate the translation or localization of mRNAs (31, 48). It is also suggested that the high GC content is due to the action of adenosine deaminase, which is implicated in the development of subacute sclerosing panencephalitis (SSPE) by introducing the biased hypermutation in the M gene of MeV (4, 5).

Using the F protein expression systems from cDNA, the F 5′ UTRs of morbilliviruses have been shown to modulate the translation efficiency of the F protein. Some studies reported that the long F 5′ UTRs of MeV, rinderpest virus, and CDV inhibit the production of the F protein (11, 13, 16, 20), whereas others showed that they enhance it (3, 16). To analyze the role of the long F 5′ UTR of MeV in virus infection, Radecke et al. generated a recombinant MeV that has a 504-nt deletion in the F 5′ UTR, using a reverse genetics system based on the Edmonston (Ed) B vaccine strain (38). They showed that there was little difference in the growth in cultured cells between the Ed virus having the

* Corresponding author. Mailing address: Department of Virology, Faculty of Medicine, Kyushu University, Fukuoka 812-8582, Japan. Phone: 81-92-642-6138. Fax: 81-92-642-6140. E-mail: mtakeda@virology.med.kyushu-u.ac.jp.

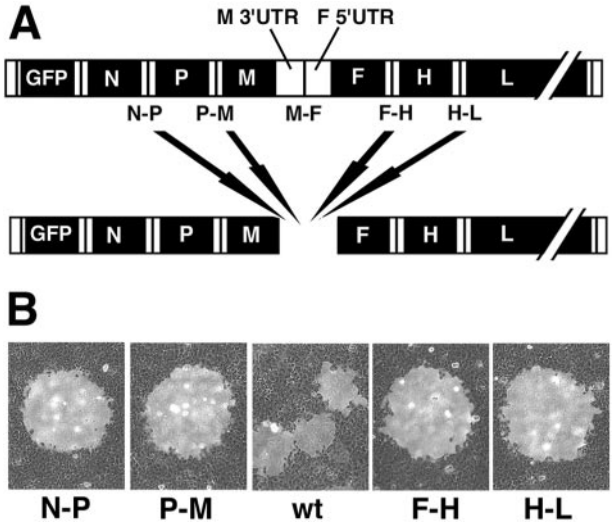

FIG. 1. Rescue of MeVs in which the long UTRs between M and F ORFs have been replaced with the counterpart short UTRs between other ORFs. (A) A diagram showing construction of mutant virus genomes. The entire region of the long UTRs between M and F ORFs (M-F) was replaced with the counterpart short UTRs between other ORFs (N-P, P-M, F-H, and H-L), as indicated by arrows. The filled areas indicate ORFs, in which encoded proteins are shown with white characters. The open areas indicate UTRs. M 3′ UTR and F 5′ UTR indicate the genomic regions corresponding to the 3′ UTR of M mRNA and 5′ UTR of F mRNA, respectively, when they are transcribed. The vertical lines in the UTRs indicate IG trinucleotides. (B) Plaques produced by the rescued viruses on Vero/hSLAM cells. Images were obtained with a light and a fluorescence microscope and merged by using Axio Vision software. The region used for the replacement in each mutant is shown at the bottom.

504-nt deletion (Δ5F-Ed) and the parental virus, suggesting that the long F 5′ UTR has no significant role in MeV replication in cultured cells (38). Valsamakis et al. analyzed the growth of the Δ5F-Ed virus in human thymus/liver implants that were engrafted into SCID mice (SCID-hu thy/liv model), and showed that the peak virus titer of the Δ5F-Ed virus was lower than that of the parental Ed virus in the SCID-hu thy/liv model (46). Their results thus suggested some role of the long F 5′ UTR in virus replication in vivo, but the molecular basis for the reduced peak virus titer of the Δ5F-Ed virus remained unknown (46). By contrast, little information exists on the possible role for the long M 3′ UTR. Wong et al. showed that, using M protein expression plasmids, at least 146 nt of the M 3′ UTR of the Ed strain could be deleted without affecting the production of the M protein (48).

Although the Ed strain is the most well-characterized MeV strain, it is known to have lost the original highly pathogenic nature of MeV during the adaptation to growth in unnatural host cells, accumulating significant mutations in the genome (42, 50). Therefore, using a reverse genetics system based on the virulent wild-type (WT) IC-B strain of MeV (41, 43), we generated a series of recombinant MeVs containing altered M 3′ UTR and F 5′ UTR. We show here that these long UTRs of the WT MeV modulate gene expression and protein production, controlling virus replication and cytopathogenicity.

MATERIALS AND METHODS

Viruses and cells. Vero cells constitutively expressing human signaling lymphocyte activation molecule (SLAM) (Vero/hSLAM) (35) were maintained in Dulbecco's modified Eagle's medium (DMEM) (ICN Biomedicals, Aurora, Ohio) supplemented with 7.5% fetal bovine serum (FBS) and 500 μg of Geneticin (G418; Nacalai Tesque, Tokyo, Japan) per ml. CHO cells constitutively expressing human SLAM (CHO/hSLAM) (44) were maintained in RPMI medium (ICN Biomedicals) supplemented with 7.5% FBS and 500 μg of G418 (Nacalai Tesque) per ml. B95a cells (25) were maintained in RPMI medium supplemented with 7.5% FBS. A549 cells constitutively expressing human SLAM (A549/hSLAM) were generated as follows. A549 cells were cotransfected with the eukaryotic expression vector pCA7, a derivative of pCAGGS (34), encoding human SLAM and the selection vector pCXN2 encoding the neomycin resistance gene, and then a clone expressing a high level of hSLAM (A549/hSLAM) was selected in the presence of G418. A549/hSLAM was maintained in RPMI medium supplemented with 7.5% FBS and 500 μg of G418 per ml. Recombinant MeVs were generated by the procedure reported recently (41). Briefly, CHO/hSLAM cells were infected with the vaccinia virus encoding T7 RNA polymerase, vTF7-3 (a gift from B. Moss), and then transfected with the full-length plasmid encoding the antigenome of MeV and three support plasmids, pCAG-T7-IC-N, pCAG-T7-IC-PΔC, and pGEMCR-9301B-L (41). On the following day, the CHO/hSLAM cells were cocultured with B95a cells to amplify the recombinant MeV rescued from the transfected full-length genome plasmid.

Construction of plasmids. All full-length genome plasmids were derived from the p(+)MV323 (43) that encodes the antigenomic full-length cDNA of the virulent IC-B strain of MeV (25, 26). The p(+)MV323-EGFP plasmid that has an additional transcriptional unit of the enhanced green fluorescent protein (EGFP) was reported previously (21). Since no available antibody against the MeV F protein was suitable for the quantification of the F protein, the influenza virus hemagglutinin (HA) epitope tag sequence (amino acid sequence is YPYDVPDYA) was added to the p(+)MV323-EGFP plasmid at the cytoplasmic region of the F protein with a flexible linker sequence (amino acid sequence is PPPELGGP) by standard molecular cloning procedures, generating p(+)MV323-EGFPtagF plasmid. All recombinant viruses used in this study possessed this modification in the F gene. Then the entire region of the long UTRs between M and F ORFs in the p(+)MV-EGFPtagF was replaced by the counterpart short UTRs between N and P (N-P), P and M (P-M), F and H (F-H), or H and L (H-L) ORFs, generating the first set of the full-length plasmids, p(+)MV-EGFPtagF-N-P, -P-M, -F-H, and -H-L, respectively (Table 1). To keep the genome length in multiples of 6, 3, 5, and 3 nt in the long UTRs remained undeleted for the generation of the p(+)MV-EGFPtagF-N-P, -P-M, and -H-L, respectively, but the hexamer position of the initiating A residue of the F mRNA was altered. The hexamer position of the initiating A residue of the F mRNA of the WT genome is 3, while those of the UTR replacement mutant N-P, P-M, F-H, and H-L virus genomes were 5, 2, 2, and 6, respectively. In the second set of the full-length genome plasmids, either or both of the 360 nt in the M 3′ UTR at nt positions 4447 through 4806 and the 540 nt in the F 5′ UTR at nt positions 4910 through 5449 were deleted from the p(+)MV-EGFPtagF plasmid, generating p(+)MV-EGFPtagF-M ΔUTR, -F ΔUTR, and –M ΔUTR+F ΔUTR, respectively. A detailed cloning procedure will be provided upon request.

Individual M and F genes were also cloned into the eukaryotic expression plasmids. The pCA7-IC-tagF+UTR was generated by cloning the entire 5′ long UTR and coding region of the IC-B F gene (nt positions 4875 through 7110) with the HA tag sequence into the pCA7 plasmid. The pCA7-IC-tagFΔUTR plasmid was generated by deleting the 579 nt (nt positions 4875 through 5453) of the 5′ long UTR from the pCA7-IC-tagF+UTR. The pCMV-IC-M+UTR plasmid was generated by cloning the entire sequence of the IC-B M gene (nt positions 3406 through 4870) between the human cytomegalovirus major immediate early

TABLE 1. Construction of the UTR replacement mutants

Full-length plasmid	Fragment removed[a]	Fragment inserted[a]
p(+)MV-EGFPtagF-N-P	4449–5457	1686–1806
p(+)MV-EGFPtagF-P-M	4451–5457	3331–3437
p(+)MV-EGFPtagF-F-H	4446–5457	7111–7270
p(+)MV-EGFPtagF-H-L	4449–5457	9125–9233

[a] Shown are nucleotide positions defining the fragments removed or inserted to construct full-length plasmids.

promoter and SV40 early mRNA polyadenylation signal sequence obtained from the pIREShyg3 plasmid (Clontech, Palo Alto, Calif.). The pCMV-IC-MΔUTR plasmid was generated by deleting the 360 nt (positions 4447 through 4806) of the 3′ long UTR from the pCMV-IC-M+UTR.

Virus titration. Monolayers of Vero/hSLAM cells on 6-well cluster plates were infected with serially diluted virus samples, and incubated for 1 h at 37°C. The inoculum was then removed, and the cells were washed with phosphate-buffered saline (PBS). The cells were overlaid with DMEM containing 5% FBS and 1% agarose. At 3 days postinfection (p.i.), PFU was determined by counting the number of plaques under a fluorescence microscope. Monolayers of Vero/hSLAM cells on 24-well cluster plates were infected with 50 μl of serially diluted virus samples, and incubated for 1 h at 37°C. After 1-h incubation, 150 μl of DMEM supplemented with 7.5% FBS and 100 μg of the fusion block peptide (Z-D-Phe-Phe-Gly) (Peptide Institute Inc., Osaka, Japan) (40) per ml was added to each well to inhibit the second round of infection by progeny virions. At 30 h p.i., the number of EGFP-expressing cells was counted under a fluorescence microscope. The number was expressed as cell infectious unit (CIU). CIU was essentially comparable to PFU.

Northern blotting. Total RNA was extracted from virus-infected cells with the TRIzol reagent (Life Technologies, Gaithersburg, MD). From the total RNA, mRNA was purified with the Oligotex-dT30 mRNA purification kit (TaKaRa Bio Inc., Shiga, Japan). Two μg of the purified mRNA was electrophoresed, transferred to polyvinylidene difluoride (PVDF) membranes (Hybond-N+; Amersham Biosciences, Piscataway, N.J.), and hybridized with ^{32}P-labeled gene specific cDNA probes synthesized with Prime-it II random primer labeling kit (Stratagene, La Jolla, Calif.) and gene specific cDNA fragments. The gene specific cDNA fragments used were at nt positions 1,134 through 1,680 for N, 1,829 through 2074 for P, 4261 through 4462 for M, 6224 through 6415 for F, 7,261 through 7586 for H, and 11,001 through 11,216 for L gene, respectively. The membranes were stripped and rehybridized with a glyceraldehyde-3-phosphate dehydrogenase (GAPDH) cDNA probe used as an internal control. Radioactivity was analyzed and quantified with a Fuji BioImager 1000 and Mac Bas software (Fuji Medical Systems, Stamford, CT).

Quantification of mRNAs by PCR. Purified mRNAs from virus-infected cells were reverse transcribed into cDNAs with iScript cDNA synthesis kit (Promega). PCR (40 to 60 cycles of 95°C for 5 s and 60°C for 20 s, or 95°C for 5 s, 58°C for 20 s, and 72°C for 20 s) was then performed with SYBR Premix Ex *Taq* (TaKaRa Bio Inc.) in capillary tubes. Primers used for this assay were 5′ GAACTCGGT ATCACTGCC 3′ and 5′ TCCTGGTAGCTCATTCTC 3′ for the N mRNA, 5′ TCCAGAGGCAACAACTTTCC 3′ and 5′ GATGGTTCCGAGGGTGAC TT 3′ for the P mRNA, 5′ GGAGTGTCTTCAATGCAAAC 3′ and 5′ TAA GGGTCACTAGCAGGTT 3′ for the M mRNA, 5′ ACAATCTGAGAGCAA GCCTG 3′ and 5′ TGAGCAATTTGAGCCCTAGC 3′ for the F mRNA, 5′ GTCAATTCTCAAACATGTCGC 3′ and 5′ TGTGACAACTCTGACCCT TTAC 3′ for the H mRNA, and 5′ CACGGTATTACATCTTCACG 3′ and 5′ GCATCTCTGTCAATTAAAGG 3′ for the L mRNA, respectively. To quantify the genome or antigenome RNAs, total RNAs from virus-infected cells were reverse transcribed with the specific primers for the 3′ genome or antigenome termini, 5′ ACCAAACAAAGTTGGGTAAG 3′ and 5′ ACCAGACAAAGC TGGGAATA 3′, respectively. PCR was then performed with SYBR Premix Ex *Taq* (TaKaRa Bio Inc.) with the speficic primer pairs that amplify the genome or antigenome termini. Primer pairs used were 5′ CAAAGTTGGGTAAGGATAT 3′ and 5′ AACTTGTGGCCGTTTACGTCG 3′ for the genome, and 5′ TTA GTCGGATACAGCGCTCTG 3′ and 5′ ATAGAAACTTCGTATTTTCA 3′ for the antigenome. Fluorescence of SYBR green was monitored at the end of each PCR cycle with the LightCycler instrument (Roche Diagnostics, Indianapolis, Ind.). Serially diluted p(+)MV323EGFPtagF plasmid was amplified in parallel with samples as a standard. GAPDH mRNA was also quantified as an internal control. Data were analyzed with the LightCycler software, version 3.5 (Roche Diagnostics).

Protein gel, antibodies, and immunoblotting. Polypeptides obtained from virus-infected cells were separated by sodium dodecyl sulfate (SDS)-polyacrylamide gel electrophoresis (PAGE) on 10% polyacrylamide-SDS gels, and blotted onto PVDF membranes (Hybond-P, Amersham Biosciences). Then, the membranes were incubated with the serum from a patient with SSPE containing high titers of antibodies against the MeV N protein (49), the rabbit anti-HA epitope-tag polyclonal antibody Y-11 (Santa Cruz Biotechnology, Santa Cruz, Calif.), and a mouse anti-MeV M protein monoclonal antibody (Chemicon, Temecula, Calif.), followed by incubation with peroxidase-conjugated anti-human, -rabbit, and -mouse secondary antibodies, respectively. Membranes were also incubated with the peroxidase-conjugated anti-HA epitope-tag monoclonal antibody 3F10 (Roche Diagnostics). After washing with PBS, the membranes were treated with the ECL plus reagent (Amersham Biosciences) and luminescence was detected and quantified with VersaDoc 3000 imager (Bio-Rad, Hercules, Calif.).

Analysis of the mRNA stability. Monolayers of Vero/hSLAM cells were transfected with the pCA7-IC-tagF+UTR, pCA7-IC-tagFΔUTR, pCMV-IC-M+UTR, or pCMV-IC-MΔUTR. At 36 h posttransfection (p.t.), total RNAs were purified from some of the monolayers, while DNAs were removed by digesting with the DNase (Toyobo, Osaka, Japan). The amounts of the M and F mRNAs, in addition to the GAPDH mRNA as internal control, were then quantified by PCR using the LightCycler instrument (Roche Diagnostics). Other monolayers were further incubated in culture medium supplemented with 10 μg of actinomycin D (Ac-D) per ml for 10 h, inhibiting the de novo RNA synthesis. After the 10-h incubation with Ac-D, the amounts of the M, F and GAPDH mRNAs remaining were quantified and compared with those at 36 h p.t. (before Ac-D treatment).

RESULTS

Rescue of recombinant MeVs in which the long stretch of UTRs between M and F ORFs was replaced with the counterpart short UTRs. In the MeV genome, the M 3′ UTR and F 5′ UTR are combined with the IG trinucleotide, composing a long stretch of UTRs of 1,012 nt in length between M and F ORFs (Fig. 1A). To test if these long UTRs have an essential role in MeV replication, we replaced the entire region of the long UTRs between M and F ORFs with the counterpart short UTRs of 107–160 nt in length present between the other pairs of ORFs (Fig. 1A). To follow the "rule of six" (10, 27) each replacement was done so as to keep the genome length in multiples of six, while the hexamer position of the initiating A residue of the F mRNA was altered by the replacement. We tested all possible ways of replacement (N-P, P-M, F-H, and H-L) (Fig. 1A), and could rescue all four viruses with efficiency similar to that obtained with the parental WT virus rescued from p(+)MV323-EGFPtagF. Notably, all four viruses were viable and even produced bigger plaques than the WT virus (Fig. 1B). These results indicate that the long UTRs between M and F ORFs per se are not indispensable for MeV replication. Also, these data suggested that the hexamer position of the initiating A residue was not critical for MeV gene expression, as found with simian virus 5 (22).

Characterization of the mutant H-L virus. We analyzed in detail one of the mutants, H-L virus (Fig. 1), in which the entire region of the long UTRs between M and F ORFs was replaced with the counterpart short UTRs between H and L ORFs. The H-L virus caused much stronger cytopathic effect (CPE) than the WT virus. In the H-L virus-infected cells, syncytia developed and spread more rapidly, accompanied with strong cell lysis (Fig. 2A). The H-L virus replicated more efficiently than the WT virus, although the peak virus titer was lower than that of the WT virus (Fig. 2B).

Figure 2C shows Northern blot detection of viral transcripts in Vero/hSLAM cells infected with the WT (lane 1) or H-L (lane 2) virus. The amounts of viral mRNAs (N, P, M, F, H, and L) and cellular GAPDH mRNA were quantified by measuring radioactivity of the hybridized ^{32}P-labeled gene specific probes. They were also quantified by reverse transcription-quantitative PCR (RT-QPCR) using the same mRNA samples (Fig. 2D). No significant difference was found between the results obtained with the two quantification methods. The amounts of viral mRNAs were generally greater in the H-L virus-infected cells than in the WT virus-infected cells (Fig. 2C and 2D). The amounts of N, P, H, and L mRNAs in the H-L

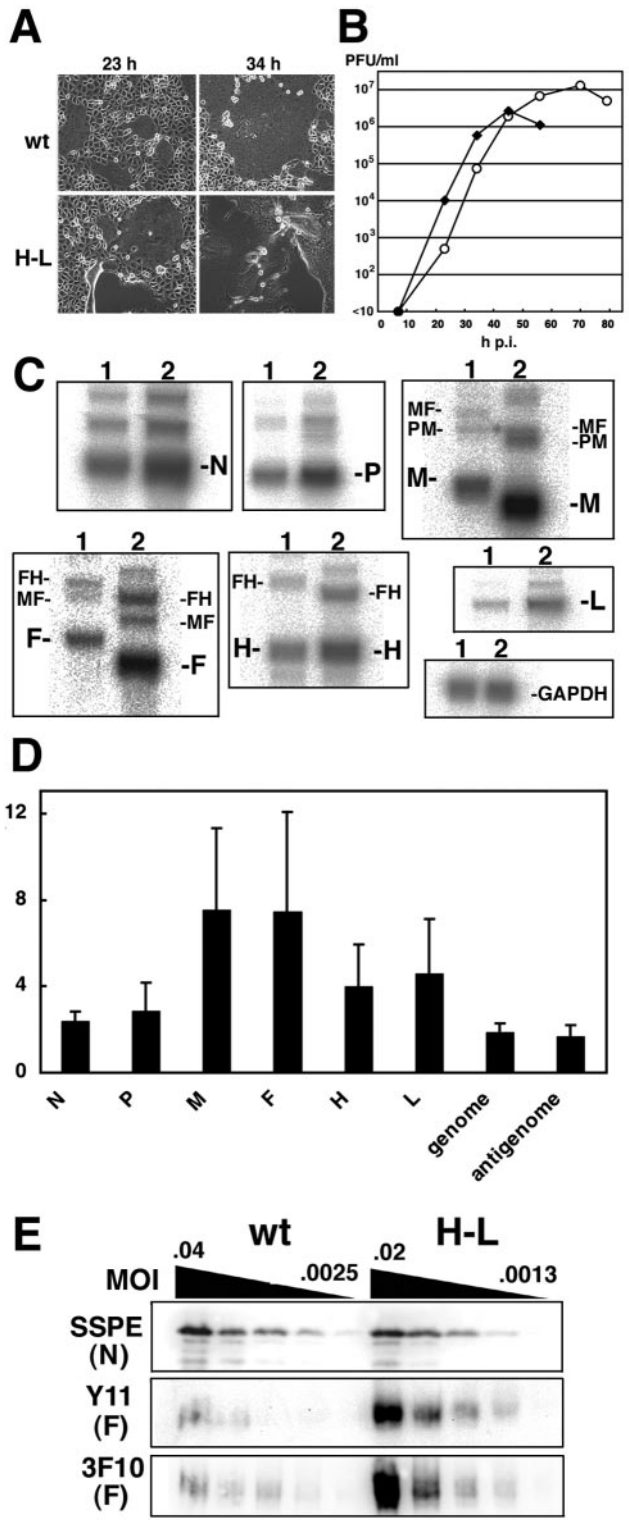

FIG. 2. Characterization of the H-L mutant virus. (A) Vero/hSLAM cells were infected with the WT and H-L viruses at an MOI of 0.01. At 23 and 34 h p.i., they were observed under a light microscope. (B) Vero/hSLAM cells were infected with the WT and H-L virus at an MOI of 0.01. At various time intervals, cells were scraped into culture media and PFU were determined on Vero/hSLAM cells. The open circles and filled diamonds indicate results with the WT and H-L viruses, respectively. (C) From the Vero/hSLAM cells infected with the WT and H-L viruses, mRNAs were purified. They were then blotted onto PDVF membrane and detected with ^{32}P-labeled DNA probes specific for the viral N, P, M, F, H, L or cellular GAPDH mRNAs. Lanes 1 and 2 contained the mRNA samples from the WT and H-L virus-infected cells, respectively. N, P, M, F, H, L, and GAPDH indicate the monocistronic mRNAs. PM, MF, and FH indicate bicistronic mRNAs that resulted from read-through at the P-M, M-F, and F-H gene boundaries, respectively. (D) Relative amounts of the mRNAs, genome, and antigenome in the H-L virus-infected cells compared with those in the WT virus-infected cells. The bar graph shows the data from the triplicate experiments. The mean ± standard deviations are shown. (E) Vero/hSLAM cells were infected with the WT and H-L viruses at different MOIs, as indicated at the top. Polypeptides obtained from the virus-infected cells at 27 h p.i. were subjected to SDS-PAGE and blotted onto PVDF membranes. The membranes were incubated with the serum from a patient with SSPE, anti-HA epitope-tag Y-11 and 3F10 antibodies, and then with the appropriate secondary antibodies conjugated with peroxidase. Membranes were treated with ECL plus reagent and luminescence was detected and quantified using a VersaDoc 3000 imager. The detected viral proteins are shown in parentheses.

virus-infected cells quantified by RT-QPCR were 2.4-, 2.9-, 4.0-, and 4.6-fold higher, respectively, than those in the WT virus-infected cells (Fig. 2D). Since the relative levels of the H and L mRNAs increased more than those of the N and P mRNAs, the reinitiation rate of transcription at the short M-F gene boundary of the H-L virus genome may be more efficient than that of the original M-F gene boundary having the long UTRs. More importantly, the increase in transcript levels was even more pronounced for the M and F mRNAs (7.6- and 7.5-fold higher than WT levels, respectively) in the H-L virus-infected cells. Amounts of the genome and antigenome were 1.9- and 1.7-fold higher, respectively, in the H-L virus-infected cells than in the WT virus-infected cells (Fig. 2D).

As reported previously (12), the amounts of bicistronic mRNAs were generally much less than those of monocistronic mRNAs (Fig. 2C). The ratios of bicistronic mRNAs to monocistronic ones were not significantly altered in the H-L virus-infected cells, as compared with the WT virus-infected cells. It was notable that the amount of the bicistronic mRNA through the F and H gene boundary (FH) was apparently greater than that of the M-F bicistronic mRNA (MF) (Fig. 2C). However, this was observed not only in the H-L virus-infected cells, but also in the WT virus-infected cells (Fig. 2C) (12). Thus, these data suggest that the long UTRs have no significant role in the M-F read-through transcription.

Next, the amounts of viral proteins in the H-L virus-infected cells were compared with those in the WT virus-infected cells (Fig. 2E). The amounts of the N and F proteins in the H-L virus-infected cells were 2.1- and 16.4-fold higher, respectively, than those in the WT virus-infected cells. The 2.1-fold increase in the N protein production could be attributed to the 2.4-fold increase in the amount of the N mRNA in the H-L virus-infected cells (Fig. 2D and 2E). However, the 16.4-fold increase in the F protein production in the H-L virus-infected cells could be only partially explained by the 7.5-fold increase in the amount of the F mRNA (Fig. 2D and 2E). These results, therefore, suggest that the increased production of the F protein in the H-L virus-infected cells was due to the increased amount as well as more efficient translation of the F mRNA

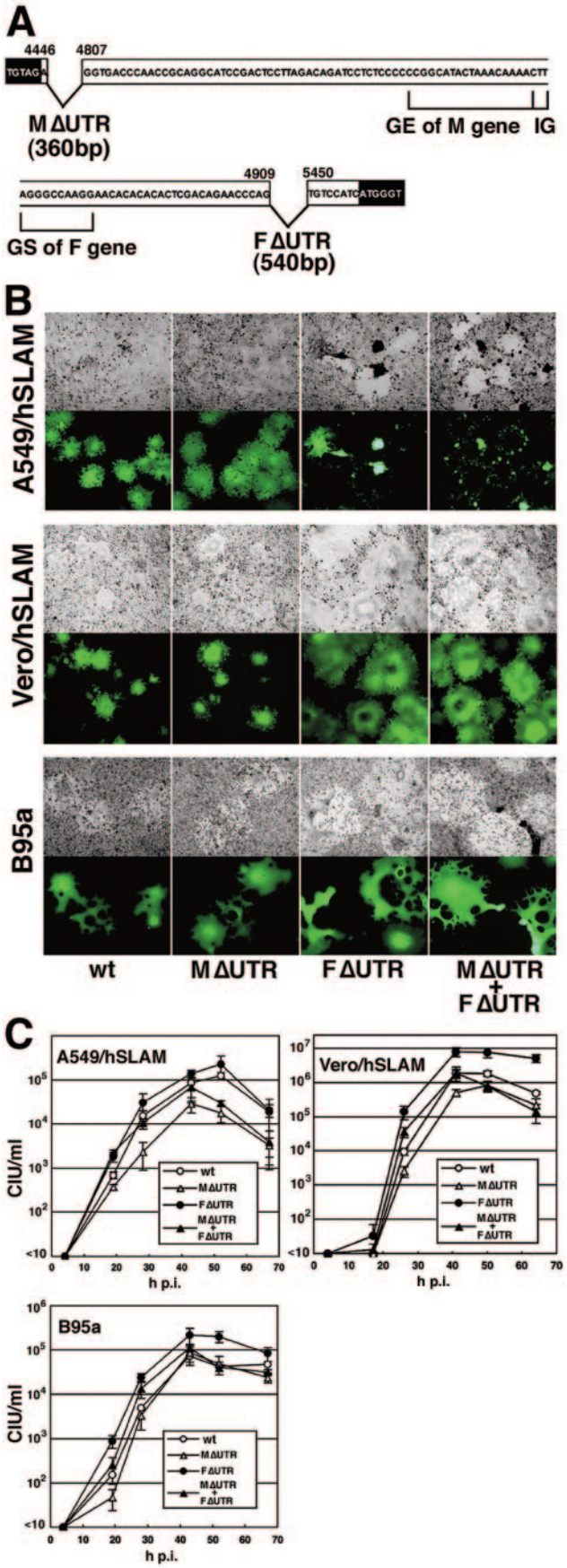

missing the long 5′ UTR, as previous reports have suggested (11, 13, 20).

Rescue and characterization of recombinant MeVs missing either or both of the long M 3′ UTR and F 5′ UTR. To analyze the respective roles of the F 5′ UTR and M 3′ UTR, another set of three mutants was generated. These mutants contain either a 360-nt deletion in the M 3′ UTR, a 540-nt deletion in the F 5′ UTR, or both of these deletions (Fig. 3A). All three mutant viruses could be rescued with efficiency similar to that of the WT virus and were viable in cultured cells. Thus, neither the long M 3′ UTR nor long F 5′ UTR proved essential for MeV replication, consistent with results shown in Fig. 1A and B. We compared CPE of the WT and mutant viruses in A549/hSLAM, Vero/hSLAM, and B95a cells (Fig. 3B). In these cells, CPE induced by the mutant virus with the 360-nt deletion in the M 3′ UTR (M ΔUTR virus) was similar to that induced by the WT virus (Fig. 3B). By contrast, the mutant virus with the 540-nt deletion in the F 5′ UTR (F ΔUTR virus) induced much stronger CPE in all three cell lines. In the F ΔUTR virus-infected cells, syncytia developed and spread more rapidly, and cells were lysed more quickly than in the WT or the M ΔUTR virus-infected cells (Fig. 3B). CPE induced by the mutant with both deletions (M ΔUTR+F ΔUTR virus) was similar to that induced by the F ΔUTR virus in all cell lines (Fig. 3B). In addition, plaques produced by the F ΔUTR or M ΔUTR+F ΔUTR virus were bigger than those produced by the WT or M ΔUTR viruses (data not shown). The first four mutant viruses having the UTR replacements also produced bigger plaques than the WT virus (Fig. 1B). These results indicate that the long F 5′ UTR, but not the long M 3′ UTR, moderates CPE, and reduces the size of the plaques produced.

Next, we compared replication kinetics of the WT, M ΔUTR, F ΔUTR, and M ΔUTR+F ΔUTR viruses in A549/hSLAM, Vero/hSLAM, and B95a cells (Fig. 3C). The long F 5′ UTR appeared to inhibit virus replication, as the F ΔUTR virus replicated more efficiently in all cell lines than the WT virus (Fig. 3C). The M ΔUTR + F ΔUTR virus also replicated more efficiently than the M ΔUTR virus (Fig. 3C). By contrast, the long M 3′ UTR seemed to promote virus replication, as the

FIG. 3. Rescue and characterization of MeVs having a 360-nt deletion in the M 3′ UTR and/or a 540-nt deletion in the F 5′ UTR. (A) A diagram showing construction of mutant virus genomes. Either or both of the 360-nt deletion in the M 3′ UTR at nt positions 4447 through 4806 (M ΔUTR) and the 540-nt deletion in the F 5′ UTR at nt positions 4910 through 5449 (F ΔUTR) were introduced into the virus genome. The filled and open areas indicate ORFs and UTRs, respectively. GE sequence of the M gene, GS sequence of the F gene, and IG trinucleotide are indicated. (B) A549/hSLAM, Vero/hSLAM, and B95a cells were infected with the WT, M ΔUTR, F ΔUTR, and M ΔUTR+F ΔUTR viruses at an MOI of 0.01. At 2 days p.i., the cells were observed under a light (upper panels) and a fluorescence (lower panels) microscope. (C) A549/hSLAM, Vero/hSLAM, and B95a cells were infected with the WT, M ΔUTR, F ΔUTR, and M ΔUTR+F ΔUTR viruses at an MOI of 0.01. At various time intervals, the cells were scraped into culture media and CIU determined on Vero/hSLAM cells. The bars indicate the mean ± standard deviations in triplicate samples. The open circles and triangles indicate results with the WT and M ΔUTR viruses, respectively. The filled circles and triangles indicate results with the F ΔUTR and M ΔUTR+F ΔUTR viruses, respectively.

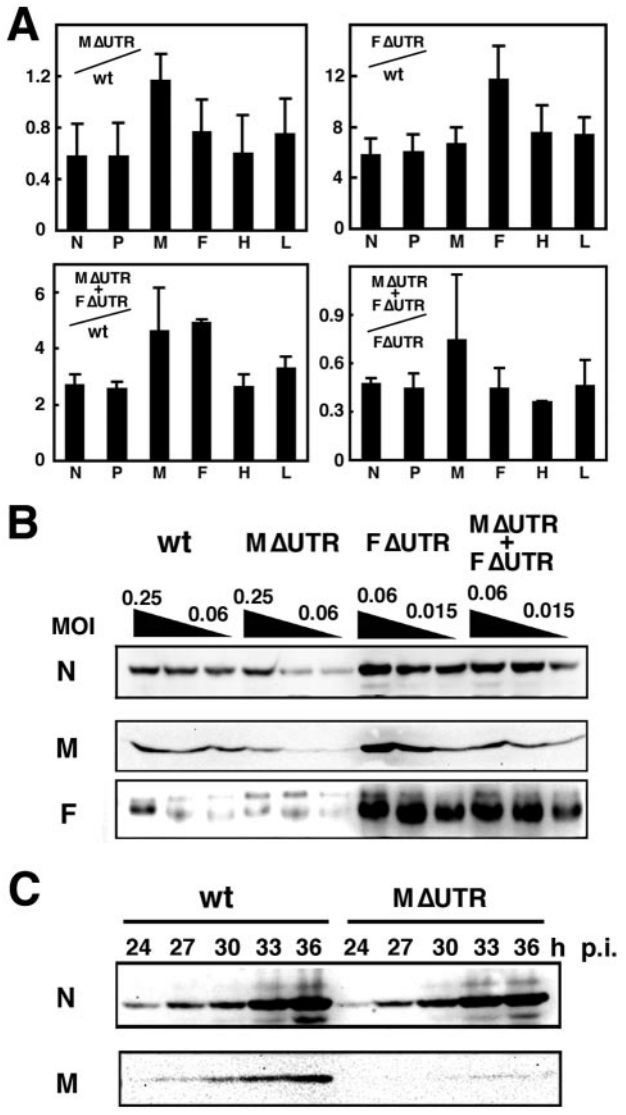

FIG. 4. Gene expression of the WT, M ΔUTR, F ΔUTR, and M ΔUTR+F ΔUTR viruses. (A) Vero/hSLAM cells were infected with the WT, M ΔUTR, F ΔUTR, and M ΔUTR+F ΔUTR viruses. At 24 h p.i., N, P, M, F, H, and L mRNAs in the virus-infected cells were quantified by RT-QPCR. Bar graphs show the amounts of the mRNAs in the M ΔUTR, F ΔUTR, and M ΔUTR+F ΔUTR virus-infected cells relative to the amounts of those mRNAs in the WT virus-infected cells (M ΔUTR/WT, F ΔUTR/WT, or M ΔUTR+F ΔUTR/WT, respectively). M ΔUTR+F ΔUTR/F ΔUTR shows the amount of the viral mRNAs in the M ΔUTR+F ΔUTR virus-infected cells relative to the amount in the F ΔUTR virus-infected cells. The bars indicate the mean ± standard error in triplicate samples. (B) Vero/hSLAM cells were infected with the WT, M ΔUTR, F ΔUTR, and M ΔUTR+F ΔUTR viruses at different MOIs, as indicated at the top. At 24 h p.i., N, M, and F proteins in the virus-infected cells were detected and quantified by immunoblotting, as described in the legend of Fig. 2E. (C) Vero/hSLAM cells were infected with the WT and M ΔUTR viruses at an MOI of 0.2. At various time intervals, N and M proteins in the virus-infected cells were detected and quantified by immunoblotting, as described in the legend to Fig. 2E.

M ΔUTR virus replicated less efficiently than the WT virus, and the M ΔUTR + F ΔUTR virus grew less efficiently than the F ΔUTR virus (Fig. 3C). The WT virus replicated as efficiently as the M ΔUTR+F ΔUTR virus, but with greatly reduced cytopathogenicity (Fig. 3B and 3C).

Gene expression of the WT, M ΔUTR, F ΔUTR, and M ΔUTR + F ΔUTR viruses. We compared the levels of viral mRNAs and proteins in the WT, M ΔUTR, F ΔUTR, and M ΔUTR+F ΔUTR virus-infected cells. At 24 h p.i., the amounts of the viral mRNAs in the WT, M ΔUTR, F ΔUTR, and M ΔUTR+F ΔUTR virus-infected Vero/hSLAM cells were analyzed by RT-QPCR. Figure 4A shows the relative amounts of N, P, M, F, H, and L mRNAs in the M ΔUTR, F ΔUTR, or M ΔUTR+F ΔUTR virus-infected cells compared with the amounts of these mRNAs in WT virus-infected cells (M ΔUTR/WT, F ΔUTR/WT, or M ΔUTR+F ΔUTR/WT), respectively. Similarly, M ΔUTR+F ΔUTR/F ΔUTR shows the relative amounts of the viral mRNAs in the M ΔUTR+F ΔUTR virus-infected cells compared with the amounts of these mRNAs in the F ΔUTR virus-infected cells. In all comparisons (M ΔUTR/WT, F ΔUTR/WT, M ΔUTR+F ΔUTR/WT, or M ΔUTR+F ΔUTR/F ΔUTR), the relative amounts of the N, P, H, and L mRNAs were more or less constant (Fig. 4A). These results suggest that neither the long M 3′ UTR nor long F 5′ UTR modulates the reinitiation rate of transcription at the M-F gene boundary. By contrast, the relative amounts of the M mRNAs increased ~1.5-fold compared with those of other mRNAs when the virus possessed the 360-nt deletion in the M 3′ UTR (M ΔUTR/WT and M ΔUTR+F ΔUTR/WT and M ΔUTR+F ΔUTR/F ΔUTR). A similar increase in the relative amount of the F mRNAs was observed when the virus contained the 540-nt deletion in the F 5′ UTR (F ΔUTR/WT and M ΔUTR+F ΔUTR/WT).

We analyzed the amounts of the N, M, and F proteins in Vero/hSLAM cells infected with the WT, M ΔUTR, F ΔUTR, or M ΔUTR+F ΔUTR viruses by immunoblotting (Fig. 4B). The amounts of the F protein in the F ΔUTR and M ΔUTR+F ΔUTR virus-infected cells were greater than those in the WT and M ΔUTR virus-infected cells, even when they were normalized with the amounts of the N protein (Fig. 4B). These results suggest that the long F 5′ UTR inhibits the F protein production, consistent with the results of the H-L virus (Fig. 2E). By contrast, the long M 3′ UTR appeared to enhance the M protein production, as the amount of the M protein in the M ΔUTR virus-infected cells normalized with the amount of the N protein was about half of that detected in the WT virus-infected cells (Fig. 4B). Similarly, the amount of the M protein in the M ΔUTR+F ΔUTR virus-infected cells was about three times less than that detected in the F ΔUTR virus-infected cells, while the amounts of the N and F proteins were comparable in those cells (Fig. 4B). These results were confirmed by a time course experiment (Fig. 4C). Vero/hSLAM cells were infected with the WT and M ΔUTR viruses, and the amounts of the N and M proteins were then analyzed at various time intervals. The production of the M protein was reduced in the M ΔUTR virus-infected cells (Fig. 4C), while the level of the M mRNA in them was similar to that of the WT virus-infected cells (Fig. 4A, M ΔUTR/WT). Thus, our results suggest that the long M 3′ UTR is required for efficient M protein translation and production.

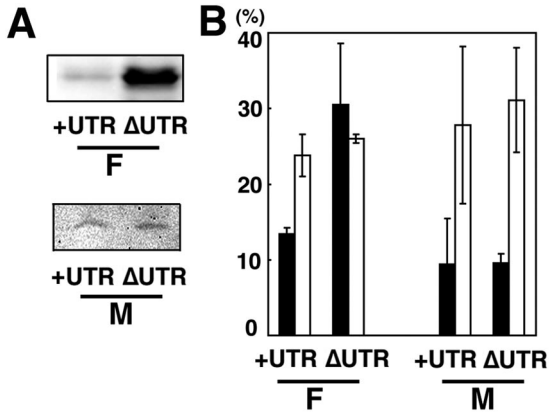

FIG. 5. Analyses of mRNA stability and protein production by a plasmid-expression system. (A) Monolayers of Vero/hSLAM cells were transfected with the pCA7-IC-tagF+UTR (F +UTR), pCA7-IC-tagFΔUTR (F ΔUTR), pCMV-IC-M+UTR (M +UTR), or pCMV-IC-MΔUTR (M ΔUTR). At 36 h p.t., M and F proteins were detected by immunoblotting. (B) To analyze the mRNA stability, the cells at 36 h p.t. were incubated in culture medium supplemented with 10 μg of Ac-D per ml for 10 h. The amounts of the M and F mRNAs in the cells before Ac-D treatment and those after 10-h incubation with Ac-D were then compared by RT-QPCR. The amount of each mRNA before Ac-D treatment was set to 100%. The bar graph shows the data of the amounts of mRNAs after 10-h incubation with Ac-D. The filled bars indicate the M and F mRNAs and open bar the GAPDH mRNA used as internal control. The mean ± standard deviations in triplicate samples are shown.

Analysis of the mRNA stability and protein production by using expression plasmids. To analyze the effect of the long UTRs on the stability of the M and F mRNAs, and production of the M and F proteins, we performed transient expression studies using eukaryotic expression plasmids. Individual mRNAs were examined in cells transfected with the plasmids with or without UTR sequence. The level of the F mRNA in the pCA7-IC-tagF+UTR-transfected cells at 36 h p.t. was ~45% of that in the pCA7-IC-tagFΔUTR-transfected cells (data not shown), while the amount of the F protein in the former was only ~20% of that in the latter (Fig. 5A). These data confirmed previous studies that the long UTR had an inhibitory role in the F protein expression, when expressed from plasmids (11, 13, 20). At 36 h p.t., de novo synthesis of mRNAs was blocked by incubating the cells with the medium supplemented with Ac-D, and the level of each mRNA remaining after 10-h incubation with Ac-D was quantified. About 25% of the cellular GAPDH mRNAs remained (Fig. 5B). The F mRNA having the 5′ long UTR, which was transcribed from the pCA7-IC-tagF+UTR, was apparently less stable than the GAPDH mRNA, only 13.4% remaining (Fig. 5B). On the other hand, the remaining level of the F mRNA lacking the long 5′ UTR derived from the pCA7-IC-tagFΔUTR was comparable to that of the GAPDH mRNA (Fig. 5B). These data indicate that the long 5′ UTR destabilizes the F mRNA. By contrast, the levels of the M mRNA and M protein at 36 h p.t. did not differ significantly between the pCMV-IC-M+UTR- and pCMV-IC-MΔUTR-transfected cells (Fig. 5A and data not shown). Also the mRNA stability was not significantly affected by the long 3′ UTR in this assay using the eukaryotic expressing plasmids (Fig. 5B). Both M mRNAs having or not having the long 3′ UTR exhibited the similar levels of stability in relation to the cellular mRNAs.

DISCUSSION

Viruses are absolute parasites of living organisms, and may have evolved to minimize the sizes of their genomes, in which the coding capacities are expanded with a variety of the coding strategies. For example, the genomes of paramyxoviruses encode three unique polypeptides (the P, V, and C proteins) in the overlapping ORFs in the P gene (30). Considering such astonishing coding strategies of these viruses, it seems unlikely that a virus would retain wasteful genome regions throughout its evolutional history. Nevertheless, morbillivirus genomes, unlike the genomes of other paramyxoviruses, have unusually long M 3′ UTRs and F 5′ UTRs (1, 2, 6, 7, 9, 14, 15, 19, 23, 32, 33, 39, 45). In this study, we showed that these long UTRs per se were not essential for MeV replication, but that alteration or deletion of these long UTRs influenced virus replication and cytopathogenicity. Viruses with a 540-nt deletion in the F 5′ UTR had enhanced replication capacity, and caused much stronger CPE in the host cells. Therefore, one explanation for the maintenance of the long F 5′ UTR during the evolution of MeV may be that the long F 5′ UTR is required to moderate cytopathogenicity of MeV at the expense of replication capacity. On the other hand, viruses with a 360-nt deletion in the M 3′ UTR had a reduced replication phenotype, suggesting that the long M 3′ UTR promotes virus replication. Consequently, by having both the long M and F UTRs, MeV may be able to replicate efficiently with reduced cytopathogenicity.

How do the long UTRs modulate virus replication and cytopathogenicity? Our results showed that the long F 5′ UTR has the capacity to decrease the F protein production. The reduced cytopathogenicity is likely a direct effect of this decreased F protein production, because the F protein is the key molecule for the virus-induced cell-to-cell fusion. Inhibition of virus replication by the long F 5′ UTR may also result from the reduced cell-to-cell fusion, which causes less efficient cell-to-cell virus transmission. Furthermore, the reduced amount of the F protein, which is a major structural glycoprotein on the virus envelope, may also affect virus assembly, resulting in poor replication. On the other hand, the long M 3′ UTR has the ability to increase the M protein production. We speculate that the increased production of the M protein directly promotes virus assembly and budding of progeny virions.

Interestingly, it has been reported that Sendai virus (SeV) and human parainfluenza virus type 1 (hPIV1) also possess strategies to inhibit production of the F protein (8, 24). Kato et al. showed that SeV inhibits production of the F protein and its downstream H and L proteins by having a unique GS signal at the F gene and thus reducing the reinitiation rate of transcription at the M-F gene boundary (24). The mutant SeV, in which the GS signal at the F gene was replaced by the common GS signal found at the P, M, and HN genes, replicated more efficiently and showed higher virulence in mice than the parental SeV (24). In spite of the apparent disadvantage of the GS signal at the F gene for virus replication in both cultured cells and animals, the sequence of the GS signal at the F gene is conserved among all known

SeV strains. The authors therefore suggested that the moderation of transcription at the F gene might be relevant to viral fitness in nature (24). The F gene of hPIV1 possesses a long 5′ UTR of 264 nt in length. Bousse et al. showed that the long UTR contributed to the read-through transcription at the M-F gene boundary, inhibiting the expression of the F gene (8). CDV also moderates the virus-induced cell fusion by having the unique amino-terminal precursor sequence of the F protein encoded in the region originally considered as a 5′ long UTR of CDV F gene (47).

In the case of MeV studied here, the relative amounts of the M and F mRNAs increased ~1.5-fold with the 360- and 540-nt deletions in the M and F UTRs, respectively. However, comparison of the amounts of N, P, H, and L mRNAs of the deletion mutants indicated that neither the long M 3′ UTR nor the long F 5′ UTR of MeV altered the reinitiation rate of transcription at the M-F gene boundary. On the other hand, the small alteration of the reinitiation rate of transcription may have occured in the H-L virus-infected cells. The *cis*-acting sequence(s) (such as, GE, IG, and GS) replaced in the H-L virus genome may be responsible for this observation, as found with SeV (24). The ~1.5-fold increase in the amounts of the F mRNA was likely due to the increase in the stability of the mRNA missing the long UTR. However, the change in the stability was not observed for the M mRNA using the plasmid-expression system. Thus, some specific mechanism(s) may operate in virus-infected cells, but not plasmid-transfected cells, which modulates the M mRNA stability or M protein production by acting on the M 3′ UTR. Alternatively, some properties, including terminal sequences, of the M mRNAs expressed from virus and plasmids may differ from each other. Further analysis is now in progress to clarify the mechanism of action of the M 3′ UTR.

In agreement with previous studies in which individual genes were expressed from plasmids (11, 13, 20), the long F 5′ UTR appeared to inhibit the F protein translation, as the ratio of the F protein production to the amount of the F mRNA was significantly higher in the absence of the long F 5′ UTR. On the other hand, our results suggested that in the virus-infected cells the long M 3′ UTR promotes the M protein translation, since the M protein production was severely restricted in the absence of the long M 3′ UTR. Lines of evidence have indicated that the 3′ and 5′ UTRs of viral and eukaryotic mRNAs have crucial roles in gene expression. They may control transcription of mRNA, and also function post-transcriptionally by determining the subcellular localization, stability, and translation efficiency of mRNAs (17, 28, 37). Our initial search using the UTR database failed to find any known motif in the MeV long UTRs (36). A detailed mapping of functional motifs in the MeV long UTRs and search for host factors that may interact with the motifs may reveal a novel strategy of MeV or cells to regulate gene expression.

In conclusion, we demonstrated that the long M 3′ UTR and long F 5′ UTR of MeV are nonessential for virus replication, but that they regulate MeV replication and cytopathogenicity by modulating the productions of the M and F proteins. By having both long M and F UTRs, MeV may replicate efficiently and minimize cytopathogenicity. We speculate that the reduction of cytopathogenicity may be advantageous for MeV fitness and survival in nature.

ACKNOWLEDGMENTS

We thank H. Minagawa for helpful discussions and T. Muta, H. Kuwata, R. Koga, and K. Takeda for technical support. We are grateful to K. Takeuchi for his contribution to the establishment of the reverse genetics of IC-B strain. We also thank T. Shima for his work at the initial stage of this study and A. P. Schmitt for critical reading and helpful comments.

This work was supported by grants from the Ministry of Education, Science, and Culture and the Ministry of Health, Labor, and Welfare of Japan, the Japan Society for the Promotion of Science, and Takeda Science Foundation.

REFERENCES

1. **Baron, M. D., L. Goatley, and T. Barrett.** 1994. Cloning and sequence analysis of the matrix (M) protein gene of rinderpest virus and evidence for another bovine morbillivirus. Virology **200:**121–129.
2. **Barrett, T., D. K. Clarke, S. A. Evans, and B. K. Rima.** 1987. The nucleotide sequence of the gene encoding the F protein of canine distemper virus: a comparison of the deduced amino acid sequence with other paramyxoviruses. Virus Res. **8:**373–386.
3. **Barrett, T., S. M. Subbarao, G. J. Belsham, and W. J. Mahy.** 1991. The molecular biology of the morbilliviruses, p. 83–102. *In* D. W. Kingsbury (ed.), The paramyxoviruses. Plenum Press, New York, N.Y.
4. **Bass, B. L.** 2002. RNA editing by adenosine deaminases that act on RNA. Annu. Rev. Biochem. **71:**817–846.
5. **Bass, B. L., H. Weintraub, R. Cattaneo, and M. A. Billeter.** 1989. Biased hypermutation of viral RNA genomes could be due to unwinding/modification of double-stranded RNA. Cell **56:**331.
6. **Bellini, W. J., G. Englund, C. D. Richardson, S. Rozenblatt, and R. A. Lazzarini.** 1986. Matrix genes of measles virus and canine distemper virus: cloning, nucleotide sequences, and deduced amino acid sequences. J. Virol. **58:**408–416.
7. **Bolt, G., M. Blixenkrone-Moller, E. Gottschalck, R. G. Wishaupt, M. J. Welsh, J. A. Earle, and B. K. Rima.** 1994. Nucleotide and deduced amino acid sequences of the matrix (M) and fusion (F) protein genes of cetacean morbilliviruses isolated from a porpoise and a dolphin. Virus Res. **34:** 291–304.
8. **Bousse, T., T. Matrosovich, A. Portner, A. Kato, Y. Nagai, and T. Takimoto.** 2002. The long noncoding region of the human parainfluenza virus type 1 F gene contributes to the read-through transcription at the M-F gene junction. J. Virol. **76:**8244–8251.
9. **Buckland, R., C. Gerald, R. Barker, and T. F. Wild.** 1987. Fusion glycoprotein of measles virus: nucleotide sequence of the gene and comparison with other paramyxoviruses. J. Gen. Virol. **68:**1695–1703.
10. **Calain, P., and L. Roux.** 1993. The rule of six, a basic feature for efficient replication of Sendai virus defective interfering RNA. J. Virol. **67:**4822–4830.
11. **Cathomen, T., C. J. Buchholz, P. Spielhofer, and R. Cattaneo.** 1995. Preferential initiation at the second AUG of the measles virus F mRNA: a role for the long untranslated region. Virology **214:**628–632.
12. **Cattaneo, R., G. Rebmann, A. Schmid, K. Baczko, V. ter Meulen, and M. A. Billeter.** 1987. Altered transcription of a defective measles virus genome derived from a diseased human brain. EMBO J. **6:**681–688.
13. **Cattaneo, R., and J. K. Rose.** 1993. Cell fusion by the envelope glycoproteins of persistent measles viruses which caused lethal human brain disease. J. Virol. **67:**1493–1502.
14. **Curran, M. D., Y. J. Lu, and B. K. Rima.** 1992. The fusion protein gene of phocine distemper virus: nucleotide and deduced amino acid sequences and a comparison of morbillivirus fusion proteins. Arch. Virol. **126:**159–169.
15. **Curran, M. D., and B. K. Rima.** 1992. The genes encoding the phospho- and matrix proteins of phocine distemper virus. J. Gen. Virol. **73:**1587–1591.
16. **Evans, S. A., G. J. Belsham, and T. Barrett.** 1990. The role of the 5′ nontranslated regions of the fusion protein mRNAs of canine distemper virus and rinderpest virus. Virology **177:**317–323.
17. **Gale, M., Jr., S. L. Tan, and M. G. Katze.** 2000. Translational control of viral gene expression in eukaryotes. Microbiol. Mol. Biol. Rev. **64:**239–280.
18. **Griffin, D. E.** 2001. Measles virus, p. 1401–1441. *In* D. M. Knipe, P. M. Howley, D. E. Griffin, R. A. Lamb, M. A. Martin, B. Roizman, and S. E. Straus (ed.), Fields virology, 4th ed. Lippincott Williams & Wilkins, Philadelphia, Pa.
19. **Haffar, A., G. Libeau, A. Moussa, M. Cecile, and A. Diallo.** 1999. The matrix protein gene sequence analysis reveals close relationship between peste des petits ruminants virus (PPRV) and dolphin morbillivirus. Virus Res. **64:**69–75.
20. **Hasel, K. W., S. Day, S. Millward, C. D. Richardson, W. J. Bellini, and P. A. Greer.** 1987. Characterization of cloned measles virus mRNAs by in vitro transcription, translation, and immunoprecipitation. Intervirology **28:**26–39.
21. **Hashimoto, K., N. Ono, H. Tatsuo, H. Minagawa, M. Takeda, K. Takeuchi, and Y. Yanagi.** 2002. SLAM (CD150)-independent measles virus entry as revealed by recombinant virus expressing green fluorescent protein. J. Virol. **76:**6743–6749.

22. **He, B., and R. A. Lamb.** 1999. Effect of inserting paramyxovirus simian virus 5 gene junctions at the HN/L gene junction: analysis of accumulation of mRNAs transcribed from rescued viable viruses. J. Virol. **73:**6228–6234.
23. **Hsu, D., M. Yamanaka, J. Miller, B. Dale, M. Grubman, and T. Yilma.** 1988. Cloning of the fusion gene of rinderpest virus: comparative sequence analysis with other morbilliviruses. Virology **166:**149–153.
24. **Kato, A., K. Kiyotani, M. K. Hasan, T. Shioda, Y. Sakai, T. Yoshida, and Y. Nagai.** 1999. Sendai virus gene start signals are not equivalent in reinitiation capacity: moderation at the fusion protein gene. J. Virol. **73:**9237–9246.
25. **Kobune, F., H. Sakata, and A. Sugiura.** 1990. Marmoset lymphoblastoid cells as a sensitive host for isolation of measles virus. J. Virol. **64:**700–705.
26. **Kobune, F., H. Takahashi, K. Terao, T. Ohkawa, Y. Ami, Y. Suzaki, N. Nagata, H. Sakata, K. Yamanouchi, and C. Kai.** 1996. Nonhuman primate models of measles. Lab. Anim. Sci. **46:**315–320.
27. **Kolakofsky, D., T. Pelet, D. Garcin, S. Hausmann, J. Curran, and L. Roux.** 1998. Paramyxovirus RNA synthesis and requirement for hexamer genome length: the rule of six revisited. J. Virol. **72:**891–899.
28. **Kozak, M.** 2004. How strong is the case for regulation of the initiation step of translation by elements at the 3′ end of eukaryotic mRNAs? Gene **343:**41–54.
29. **Lamb, R. A., and D. Kolakofsky.** 2001. Paramyxoviridae: the viruses and their replication, p. 1305–1340. *In* D. M. Knipe, P. M. Howley, D. E. Griffin, R. A. Lamb, M. A. Martin, B. Roizman, and S. E. Straus (ed.), Fields virology, 4th ed. Lippincott Williams & Wilkins, Philadelphia, Pa.
30. **Lamb, R. A., and R. G. Paterson.** 1991. The nonstructural proteins of paramyxoviruses, p. 181–214. *In* D. W. Kingsbury (ed.), The paramyxoviruses. Plenum Press, New York, N.Y.
31. **Liermann, H., T. C. Harder, M. Lochelt, V. von Messling, W. Baumgartner, V. Moennig, and L. Haas.** 1998. Genetic analysis of the central untranslated genome region and the proximal coding part of the F gene of wild-type and vaccine canine distemper morbilliviruses. Virus Genes **17:**259–270.
32. **Limo, M., and T. Yilma.** 1990. Molecular cloning of the rinderpest virus matrix gene: comparative sequence analysis with other paramyxoviruses. Virology **175:**323–327.
33. **Meyer, G., and A. Diallo.** 1995. The nucleotide sequence of the fusion protein gene of the peste des petits ruminants virus: the long untranslated region in the 5′-end of the F-protein gene of morbilliviruses seems to be specific to each virus. Virus Res. **37:**23–35.
34. **Niwa, H., K. Yamamura, and J. Miyazaki.** 1991. Efficient selection for high-expression transfectants with a novel eukaryotic vector. Gene **108:** 193–199.
35. **Ono, N., H. Tatsuo, Y. Hidaka, T. Aoki, H. Minagawa, and Y. Yanagi.** 2001. Measles viruses on throat swabs from measles patients use signaling lymphocytic activation molecule (CDw150) but not CD46 as a cellular receptor. J. Virol. **75:**4399–4401.
36. **Pesole, G., S. Liuni, G. Grillo, F. Licciulli, F. Mignone, C. Gissi, and C. Saccone.** 2002. UTRdb and UTRsite: specialized databases of sequences and functional elements of 5′ and 3′ untranslated regions of eukaryotic mRNAs. Update 2002. Nucleic Acids Res. **30:**335–340.
37. **Pesole, G., F. Mignone, C. Gissi, G. Grillo, F. Licciulli, and S. Liuni.** 2001. Structural and functional features of eukaryotic mRNA untranslated regions. Gene **276:**73–81.
38. **Radecke, F., P. Spielhofer, H. Schneider, K. Kaelin, M. Huber, C. Dotsch, G. Christiansen, and M. A. Billeter.** 1995. Rescue of measles viruses from cloned DNA. EMBO J. **14:**5773–5784.
39. **Richardson, C., D. Hull, P. Greer, K. Hasel, A. Berkovich, G. Englund, W. Bellini, B. Rima, and R. Lazzarini.** 1986. The nucleotide sequence of the mRNA encoding the fusion protein of measles virus (Edmonston strain): a comparison of fusion proteins from several different paramyxoviruses. Virology **155:**508–523.
40. **Richardson, C. D., A. Scheid, and P. W. Choppin.** 1980. Specific inhibition of paramyxovirus and myxovirus replication by oligopeptides with amino acid sequences similar to those at the N-termini of the F1 or HA2 viral polypeptides. Virology **105:**205–222.
41. **Takeda, M., S. Ohno, F. Seki, K. Hashimoto, N. Miyajima, K. Takeuchi, and Y. Yanagi.** 2005. Efficient rescue of measles virus from cloned cDNA using SLAM-expressing Chinese hamster ovary cells. Virus Res. **108:**161–165.
42. **Takeda, M., T. Sakaguchi, Y. Li, F. Kobune, A. Kato, and Y. Nagai.** 1999. The genome nucleotide sequence of a contemporary wild strain of measles virus and its comparison with the classical Edmonston strain genome. Virology **256:**340–350.
43. **Takeda, M., K. Takeuchi, N. Miyajima, F. Kobune, Y. Ami, N. Nagata, Y. Suzaki, Y. Nagai, and M. Tashiro.** 2000. Recovery of pathogenic measles virus from cloned cDNA. J. Virol. **74:**6643–6647.
44. **Tatsuo, H., N. Ono, K. Tanaka, and Y. Yanagi.** 2000. SLAM (CDw150) is a cellular receptor for measles virus. Nature **406:**893–897.
45. **Tsukiyama, K., Y. Yoshikawa, and K. Yamanouchi.** 1988. Fusion glycoprotein (F) of rinderpest virus: entire nucleotide sequence of the F mRNA, and several features of the F protein. Virology **164:**523–530.
46. **Valsamakis, A., H. Schneider, P. G. Auwaerter, H. Kaneshima, M. A. Billeter, and D. E. Griffin.** 1998. Recombinant measles viruses with mutations in the C, V, or F gene have altered growth phenotypes in vivo. J. Virol. **72:**7754–7761.
47. **von Messling, V., and R. Cattaneo.** 2002. Amino-terminal precursor sequence modulates canine distemper virus fusion protein function. J. Virol. **76:**4172–4180.
48. **Wong, T. C., G. Wipf, and A. Hirano.** 1987. The measles virus matrix gene and gene product defined by in vitro and in vivo expression. Virology **157:** 497–508.
49. **Yanagi, Y., B. A. Cubitt, and M. B. A. Oldstone.** 1992. Measles virus inhibits mitogen-induced T cell proliferation but does not directly perturb the T cell activation process inside the cell. Virology **187:**280–289.
50. **Yanagi, Y., N. Ono, H. Tatsuo, K. Hashimoto, and H. Minagawa.** 2002. Measles virus receptor SLAM (CD150). Virology **299:**155–161.